



(Zn, Mg)O/ZnO-based heterostructures grown by molecular beam epitaxy on sapphire: Polar vs. non-polar

J.-M. Chauveau^{a,b,*}, C. Morhain^a, M. Teisseire^a, M. Laügt^a, C. Deparis^a, J. Zuniga-Perez^{a,b}, B. Vinter^{a,b}

^a Centre de Recherche sur l'HétéroEpitaxie et ses Applications (CRHEA-CNRS), Rue Bernard Gregory, F-06560 Valbonne, Sophia Antipolis, France

^b Physics Department, University of Nice Sophia Antipolis, Parc Valrose, F-06103 Nice, France

ARTICLE INFO

Available online 29 August 2008

Keywords:

ZnO
Non-polar
Quantum wells

ABSTRACT

Zinc oxide (ZnO) has recently attracted considerable attention because of its unique physical properties and its potential applications in the blue and UV spectral range. Up to now, ZnO-based heterostructures have mostly been grown in a *c*-orientation. The growth of non-polar layers along the *a*-direction $[1\bar{1}\bar{2}0]$ has been proposed to avoid any built-in electric fields in the *c*-direction. Polar and non-polar quantum wells (QWs) embedded in (Zn, Mg)O barriers were grown on an optimized buffer. We compare the photoluminescence (PL) emission of *a*- and *c*-oriented QWs. From this comparison, we demonstrate that the QWs exhibit confinement but no indication of quantum confined Stark effect, contrary to what is observed in *c*-oriented structures. In the non-polar orientation, it is shown that the thermal quenching is not related to the thermal escape of excitons from the ZnO area, since the calculated activation energies are much lower.

© 2008 Elsevier Ltd. All rights reserved.

1. Introduction

Zinc oxide (ZnO) is a wide band-gap semiconductor with unique physical properties and a wide range of potential applications. It has already been used for applications such as sensors, transparent coating for solar cells and acoustic devices. ZnO has also recently attracted considerable interest for efficient ultraviolet LEDs and laser devices. Indeed, it is an excellent candidate for high-temperature and high-efficiency optoelectronic applications owing to its large exciton binding energy (60 meV), the largest among conventional semiconductors. Since the exciton binding energy can be further increased to 100 meV in quantum wells (QWs) [1,2], growing ZnO-based heterostructures is of particular interest for optoelectronic devices. With the incorporation of Mg into ZnO, the band gap of ZnO can be increased by 20 meV per percent of Mg [3,4]. (Zn, Mg)O is then a suitable alloy to use as confinement barrier layers of ZnO QWs. Several studies have been published on ZnO/(Zn, Mg)O QWs prepared by different growth methods such as pulsed laser deposition [5,6], metal-organic epitaxial methods [7], or molecular beam epitaxy (MBE) [8,9]. But until now (Zn, Mg)O-based heterostructures have mostly been grown in the $[0001]$ direction, a polar orientation, in which the magnitude of the internal electric

field can reach 1 MV/cm for (Zn, Mg)O/ZnO QWs [10]. The large built-in electric field results in a significant separation of electrons and holes in active layers [11], very long carrier lifetimes and hence very poor light emission efficiencies [12]. The growth on non-polar surfaces such as the *A*-plane $(1\bar{1}\bar{2}0)$ or the *M*-plane $(1\bar{1}00)$ have therefore been proposed to avoid any built-in electric fields and non-polar QWs have already been demonstrated in GaN-based non-polar heterostructures [13].

In this paper, we report on a comparison between polar and non-polar ZnO and (Zn, Mg)O/ZnO heterostructures grown by plasma-assisted MBE on different sapphire substrates. In this paper, we discuss two orientations: $[0001]$, (*c*-orientation) and $[1\bar{1}\bar{2}0]$ (*a*-orientation).

First of all we studied the detail growth and surface properties of non-polar ZnO. Next we present a comparative study of the photoluminescence (PL) properties. The last section is dedicated to the optical properties on the QWs. In that section, we demonstrate the absence of quantum confined Stark effect in non-polar (Zn, Mg)O/ZnO QWs heterostructures. We shall also discuss the actual limitations of the non-polar orientations.

2. Experimental details

The polar samples were grown on 2" sapphire substrates in a Riber Epineat MBE system equipped with conventional effusion cells for elemental Zn and Mg. Atomic oxygen was supplied via an Addon radio-frequency (*rf*) plasma cell using a *rf* power of 320 W. The growth temperature (T_G) (T_{gr}) was controlled by a

* Corresponding author at: Centre de Recherche sur l'HétéroEpitaxie et ses Applications (CRHEA-CNRS), Rue Bernard Gregory, F-06560 Valbonne, Sophia Antipolis, France. Tel.: +33 4 93 95 78 23; fax: +33 4 93 95.

E-mail address: jmc@crhea.cnrs.fr (J.-M. Chauveau).

thermocouple placed behind the substrate and by an infrared pyrometer. The growth rate is monitored by *in-situ* reflectivity. The Mg content was varied by changing the temperature of the Mg effusion cell and *ex-situ* measured by energy dispersive spectroscopy (EDS) in a scanning electron microscope. *Ex-situ* surface morphology was investigated by means of atomic force microscopy (AFM). The structural properties were investigated by high-resolution X-ray diffraction (HRXRD) experiments. Regarding PL spectroscopy, the samples were mounted in a closed-cycle cryostat and were excited using the 244 nm line of a frequency-doubled Ar laser. The PL signal was dispersed through a 64 cm focal length monochromator equipped with a 1200 gr/mm grating. The PL intensity was measured using a GaAs PM tube connected to a lock-in amplifier. The chopping frequency was set at 220 Hz.

3. Growth details

3.1. Polar structures

The growth of polar ZnO was achieved on *c*-oriented sapphire substrates. Prior to the growth of the active layers, a ZnO template was deposited at a growth temperature (T_G) of 520 °C and a growth rate of 0.45 $\mu\text{m}/\text{h}$. The QWs structures consist in the growth of a 0.2 μm -thick (Zn, Mg)O barrier layer, a ZnO QW and a 0.1 μm (Zn, Mg)O cap layer. The initial stage of the growth is 3D growth mode due to the large mismatch between ZnO and sapphire, followed by a 2D growth mode after coalescence [Viguié]. Although the optimum temperature for growing ZnO is found to be $T_G = 520^\circ\text{C}$, the (Zn, Mg)O growth should be performed at a much lower temperature ($T_G = 400^\circ\text{C}$) in order to avoid formation of facets [9]. The thickness of the QWs was varied from 1.6 to 9.5 nm, as verified using transmission electron microscopy.

3.2. Non-polar structures

The growth of non-polar ZnO heterostructures is achieved on R-Sapphire. Prior to growth, the sapphire substrates were exposed to an O beam after thermal cleaning. Then a ZnO buffer layers was grown at 400 °C and annealed at 600 °C for 10 min in order to smooth the surface as observed by reflection high-energy electron diffraction (RHEED). Fig. 1(a) shows AFM image from a ZnO buffer after 2 min growth. The initial growth is not 3D as observed in *c*-oriented layer [14]. Stripes along the in-plane *c*-direction are clearly observed. This is also confirmed by *in-situ* RHEED experiment, in which the anisotropy is clearly observed (Fig. 1(b) and (c)).

Buffer layers with low composition of Co ($\sim 1\%$) were then used in order to significantly improve the surface morphology [15].

Fig. 2(a) and (b) exhibits the effect of Co incorporation on the surface morphology. We have found that the incorporation of low content Co may stabilize the (11 $\bar{2}$ 0) face since the facets observed in Fig. 2(b) vanish, resulting in a surface roughness of ~ 3 nm (Fig. 2(b)). This effect is also observed *in-situ* during the growth by RHEED pattern in which the facets are completely removed and streaky features show up. The Cobalt incorporation may also influence the surface migration because the surface anisotropy is reduced and the growth fronts along the *c*-direction are less visible in Fig. 2(b). Note that it is possible to maintain a 2D growth mode during the whole growth process although the mismatch is still large.

Before growing the (Zn, Mg)O/ZnO active layers, a (Zn, Co)O buffer layer of various thickness was therefore systematically inserted in order to improve the surface morphology, in order to enhance the strain relaxation as well as to limit the UV luminescence from the buffer layer.

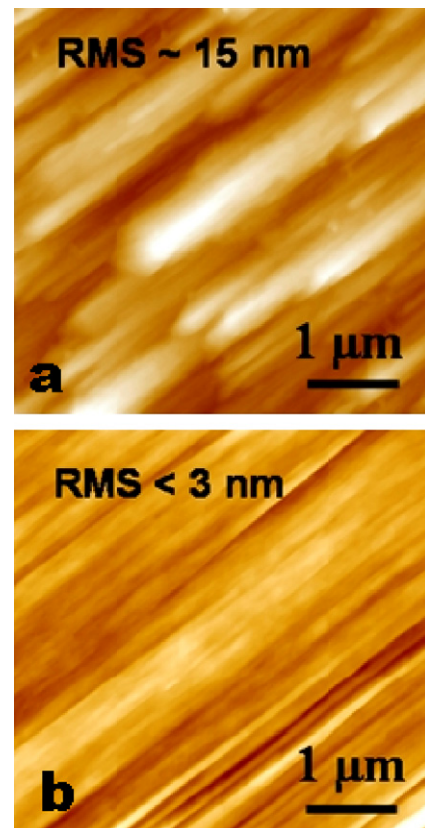


Fig. 2. AFM images taken from (a) 1 μm -thick A-plane ZnO and (b) 1 μm -thick A-plane (Zn, Co)O with 1% Co, grown under the same conditions.

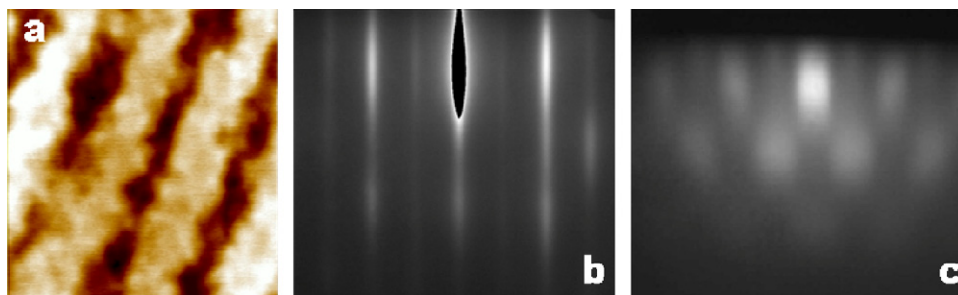


Fig. 1. (a) $2 \times 2 \mu\text{m}^2$ AFM image taken from a (Zn, Co)O buffer after 2 min growth (12 nm). 0.5 nm height stripes elongated towards the in-plane *c*-direction are observed. (1b) and (1c) RHEED patterns taken along the [0001] and [10 $\bar{1}$ 0] directions, respectively.

Download English Version:

<https://daneshyari.com/en/article/542476>

Download Persian Version:

<https://daneshyari.com/article/542476>

[Daneshyari.com](https://daneshyari.com)